Environmental Science & Technology

Article

Cite This: Environ. Sci. Technol. 2018, 52, 9079−9086

pubs.acs.org/est

Quantification of SO_2 Oxidation on Interfacial Surfaces of Acidic Micro-Droplets: Implication for Ambient Sulfate Formation

Hui-Ming Hung,*[,†] Mu-Ni Hsu,[‡] and Michael R. Hoffmann[§]

[†]Department of Atmospheric Sciences, National Taiwan University No. 1, Sec. 4, Roosevelt Road, Taipei 10617 Taiwan

[‡]National Chung-Shan Institute of Science & Technology, Taoyuan City 32557, Taiwan

[§]Linde Center for Global Environmental Science, California Institute of Technology Linde-Robinson Laboratory Pasadena, California 91125, United States

ABSTRACT: Sulfate formation on the surface of aqueous microdroplets was investigated using a spray-chamber reactor coupled to an electrospray ionization mass spectrometer that was calibrated using $Na_2SO_4(aq)$ as a function of pH. The observed formation of $SO_3^{-\bullet}$, $SO_4^{-\bullet}$, and HSO_4^- at pH < 3.5 without the addition of other oxidants indicates that an efficient oxidation pathway takes place involving direct interfacial electron transfer from SO_2 to O_2 on the surface of aqueous microdroplets. Compared to the well-studied sulfate formation kinetics via oxidation by $H_2O_2(aq)$, the interfacial SO_4^{2-} formation rate on the surface of microdroplets was estimated to be proportional to the collision frequency of SO_2 with a pH-dependent efficiency factor of $5.6 \times 10^{-5}[H^+]^{3.7}/([H^+]^{3.7}+10^{-13.5})$. The rate via the acidic surface reactions is approximately 1−2 orders of magnitude higher than that by $H_2O_2(aq)$ for a 1.0 ppbv concentration of $H_2O_2(g)$ interacting with 50 $\mu g/m^3$ of aerosols. This finding highlights the relative importance of the interfacial SO_2 oxidation in the atmosphere. Chemical reactions on the aquated aerosol surfaces are overlooked in most atmospheric chemistry models. This interfacial reaction pathway may help to explain the observed rapid conversion of SO_2 to sulfate in mega-cities and nearby regions with high PM2.5 haze aerosol loadings.

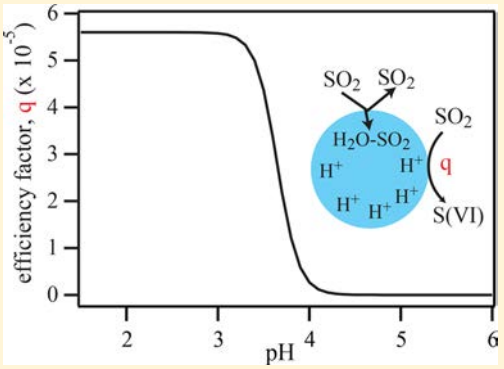

1. INTRODUCTION

Sulfate is a major inorganic component found in ambient aerosol particles.[1,2] In addition, sulfate plays an important role in cloud and haze aerosol formation due to its high hygroscopicity and its role as a cloud condensation nucleus (CCN).[3−5] Our current understanding of sulfate production in the atmosphere is that it occurs mainly via the oxidation of SO_2 with dissolved H_2O_2, O_3, R−O−OH, OH radical, oxides of nitrogen, and by O_2 in noncatalytic or catalytic pathways involving Fe(II/III) and Mn(II/III).[2,5,6] In our previous report on SO_2 and water droplet reactions using an electrospray ionization mass spectrometer (ESI-MS), a new mechanism involving the air−water interfacial oxidation of SO_2 on the surface of acidic droplets was reported.[7] The interfacial SO_2 oxidation pathway by O_2 involves the formation of $SO_3^{-\bullet}$ and $SO_4^{-\bullet}$ radicals as reaction intermediates leading to a free radical chain reaction that is often observed in catalytic SO_2 oxidation in bulk aqueous solution as initiated by transition metal ions:[8,9]

$$SO_3^{-\bullet} + O_2 \rightarrow SO_5^{-\bullet} \quad (1)$$

$$SO_5^{-\bullet} + HSO_3^- \rightarrow HSO_5^- + SO_3^{-\bullet} \quad (2)$$

$$SO_4^{-\bullet} + HSO_3^- \rightarrow HSO_4^- + SO_3^{-\bullet} \quad (3)$$

$$HSO_4^- + SO_5^{-\bullet} \rightarrow SO_4^{-\bullet} + SO_5^{2-} + H^+ \quad (4)$$

$$SO_5^{-\bullet} + SO_5^{-\bullet} \rightarrow 2SO_4^{-\bullet} + O_2 \quad (5)$$

The noncatalyzed oxidation of S(IV) by O_2 was mainly carried out by purging air or O_2 into a salt solution containing HSO_3^-/SO_3^{2-} or by exposing either air or O_2 to droplets containing of S(IV) ions. The S(VI) formation rate was determined to be proportional to $[SO_3^{2-}][H^+]^{0.5}$.[9−12] Radojevic concluded that the noncatalyzed oxidation by O_2 was not significant for ambient SO_2 conversion as compared to other aqueous-phase oxidation pathways.[11] However, the lower reported activation energy for HSO_3^- + O_2 under acidic conditions of 1.7 kcal mol^{-1} for pH < 7 vs 21.3 kcal mol^{-1} for the pH range of 7 ≤ pH ≤ 9.5,[8,9] suggests that an efficient oxidation pathway under acidic conditions may still be important. Furthermore, the experimental setup of purging oxygen gas into solution may limit the available surface area for interfacial contact. The reported oxidation via the heterogeneous reactions of $SO_2(g)$ on the surfaces of acidic droplets[7] appears to be much faster than alternative oxidation pathways under the same conditions. The observed gas−liquid interfacial surface reactions for $SO_2(g)$ are most likely initiated by a

Received: March 14, 2018
Revised: July 5, 2018
Accepted: July 24, 2018
Published: July 24, 2018

DOI: 10.1021/acs.est.8b01391
Environ. Sci. Technol. 2018, 52, 9079−9086

similar pathway as the noncatalyzed oxidation of S(IV) in aqueous solution by O_2 reported before[8,9] but with an experimental setup approaching the real environment, i.e., the gas phase reactants (i.e., oxidant and reductant) reacting at the gas−liquid interfacial layer of water on aquated aerosol particles.

Most atmospheric chemistry models currently underestimate sulfate formation; this is likely due to lower actual emissions of SO_2, less direct emission of sulfate, or possibly missing oxidation pathways.[13−15] Wang et al.[13] reported that the missing S(IV) to S(VI) chemical conversion processes can compensate for the underestimation of formed sulfate more effectively than assuming enhanced SO_2 emission rates. There are several possible reaction pathways reported recently that could compensate for the deviation between models and field observations including pathways involving NO_2,[5,16] dust +HNO_3[17] and HONO.[18] The reaction of dust particles with HNO_3 leads to the formation of nitrate salts, which lower the deliquescence relative humidity leading to more aqueous droplets that, in turn, leads to an increased uptake of SO_2. Even though dust particles may provide a higher pH environment for more efficient SO_2 uptake, the conversion rate of SO_2 to sulfate is much slower than nitrate formation due to nitric acid scavenging on the dust particles.[17,19] Under higher pH conditions, the oxidation of S(IV) by NO_2 would become more important for aerosols.[5,16] In spite of alternative theories as to various contributions to S(VI) loading, there appear to be additional unidentified pathways or mechanisms that could account for the higher sulfate levels and faster formation rates as observed in severe haze aerosol events.[13,14] We had previously shown that chemical reactions at the air−water interface of microdroplets may provide additional reaction pathways for chemical conversions in the atmosphere.[7,20,21] However, specific kinetic parameters are needed to quantitatively confirm the roles of interfacial heterogeneous gas−liquid reaction pathways.

Herein, we report on the kinetics of $SO_2(g)$ oxidation on the surface of micrometer-sized droplets based on the comparison of experimental conditions at various H_2O_2 concentrations in the aqueous phase as a function of pH with the well-studied oxidation kinetics of SO_2 by H_2O_2. The derived pH-dependent rate efficiency on droplet surfaces was extended using a box model for a given ambient aerosol condition to illustrate the importance of this mechanism as compared with the well-known S(IV) oxidation by H_2O_2 in the aqueous phase.[6,22]

2. EXPERIMENTAL METHODS AND DATA ANALYSIS

An electrospray ionization mass spectrometer (Bruker Daltonics Esquire 3000 Plus Ion Trap Mass Spectrometer), ESI-MS, with an attached reaction chamber as shown in Figure 1 was used throughout this study similar to the system previously described.[7] Chemical reagents were used as-received including sulfurous acid solution (Kanto Chemical Co., Inc., ≥5% in water), HCl (J. T. Baker, 36.5−38.0% in water), Na_2SO_4 (Sigma-Aldrich, ≥ 99%), and H_2O_2 (Sigma-Aldrich, 30% in water). Solutions were prepared with Milli-Q water (18.2 MΩ-cm at 25 °C) to achieve the desired concentrations.

2.1. pH Adjustment and Gas Flow Control. A flow of aqueous microdroplets into the reaction chamber was generated from solutions at a flow rate of 5 μL min^{-1} using a nebulizer at a pressure of 20 psi. The dry carrier gas was set to a flow rate of 6 L min^{-1} at a temperature of 280 °C while the capillary voltage was kept constant for the quantitative

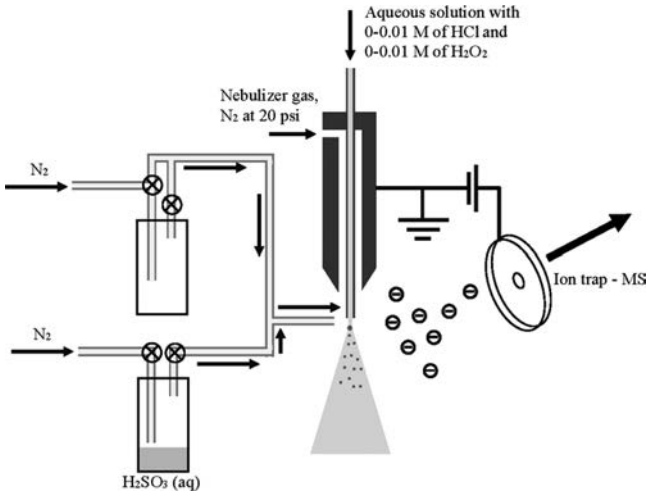

Figure 1. A schematic diagram of the experimental setup with SO_2 introduced from the gas phase and H_2O_2 and HCl introduced in the aqueous phase.

analyses among different experiments. The initial pH of bulk aqueous solutions was prepared over a range of 2 to 5.6 using HCl. Gas-phase species were introduced by flowing dry nitrogen through the top surface of the target solutions to transfer the gaseous vapor into the spray chamber with a total flow rate of 300 mL min^{-1}. For example, SO_2 was introduced by passing 150 mL min^{-1} of N_2 through a bottle partially filled with ≥5% H_2SO_3 solution received without further treatment. The other N_2 flow was applied to maintain the total flow rate as 300 mL min^{-1}. The gas-phase concentration inside the bottle was estimated using the Henry's Law constant under the assumption of equilibrium between the gas phase and the aqueous solution. The gas mixture containing SO_2 was introduced into the spray chamber through a 1/32″-ID Teflon tube nearby the nozzle as a crossing flow passing through to the region of the Taylor cone and micrometer-sized jet of the nozzle to react with the aqueous solution as shown in Figure 1. The actual gas concentration should be lower than this estimated value due to the possible mass-transfer limitations of the gas volatilization from H_2SO_3 aqueous solution. The concentration of SO_2 in the flow before further dilution was estimated as $\sim 2 \times 10^5$ ppm if the equilibrium were reached. In the nebulizer chamber, the SO_2 concentration was further diluted by the nebulizer gas and the dry carrier gas to be less than 10^4 ppm, which is significantly higher than the ambient conditions but was required to receive significant intensity due to the short reaction time (∼ ms) with the droplets for the current setup. The intensity of selected peaks was normalized with the bisulfate peak for solutions without H_2O_2 at pH = 4 daily to correct the daily fluctuation of the instrument response and possible SO_2 variations. Because the ion response is likely to vary with pH, the observed sulfate quantity was estimated based on the interpolation of bisulfate (m/e = 97) intensity, I_{97}, calibrated using Na_2SO_4(aq) over a range of 0 to 0.8 mM under different pH conditions.

2.2. Quantification of the Sulfate Formation Rate. The sulfate formation via the reaction of bisulfite with H_2O_2 in the aqueous phase proceeds as follows:[5,6,22]

$$HSO_3^- + H_2O_2 \rightleftharpoons HOOSO_2^- + H_2O \quad (6)$$

$$HOOSO_2^- + H^+ \rightarrow HSO_4^- + H^+ \quad (7)$$

DOI: 10.1021/acs.est.8b01391
Environ. Sci. Technol. 2018, 52, 9079−9086

in which bisulfite reacts with H_2O_2 to form peroxymonosulfite, $HO_2SO_2^-$, a transient intermediate, which forms bisulfate through a general acid- or proton-catalyzed rearrangement. The sulfate formation rate via H_2O_2 oxidation is determined using the following equation:[5,22]

$$R_{H_2O_2,droplet} = 7.45 \times 10^7 [HSO_3^-][H_2O_2(aq)]([H^+]/(1 + 13 \times [H^+]))(M/s) \quad (8)$$

Such reaction happens at the aqueous phase and requires the presence of HSO_3^-, which is estimated based on the uptake of SO_2 on the droplets with the dissociation rate and equilibrium constants given in our previous study[7] and also briefly summarized in section 2.3. The concentration of formed sulfate via the oxidation of SO_2 by $H_2O_2(aq)$ was monitored for $[H_2O_2(aq)]$ in a range of 0 to 5 mM. The increased acidity due to the formation of bisulfate may lower the response of the peak at m/e = 97, but enhance the interfacial oxidation of SO_2 with O_2. For simplicity, the effect of the increased acidity was assumed to be negligible.

2.3. Simulation of Gaseous SO_2 Uptake and Oxidation. The simulation of SO_2 uptake and oxidation was performed using Mathematica (Wolfram) by taking in to account the mass transfer of $SO_2(g)$ on the droplets, which can either be oxidized on the acidic surface or further accommodated into the aqueous phase and coupled with the subsequent dissociation of aquated (i.e., hydrated) $SO_2(aq)$ or $SO_2{\cdot}H_2O$ in eqs 9−11 as given in our previous study.[7]

$$SO_{2(g)} + H_2O \rightleftarrows H_2O{\cdot}SO_{2(aq)}, \quad K_H = 1.3\ M\ bar^{-1} \quad (9)$$

$$H_2O{\cdot}SO_{2(aq)} \rightleftarrows HSO_3^- + H^+, \quad K_{a1} = k_1/k_{-1} = 10^{-1.8}\ M \quad (10)$$

$$HSO_3^- \rightleftarrows SO_3^{2-} + H^+, \quad K_{a2} = k_2/k_{-2} = 10^{-7.2}\ M \quad (11)$$

To simplify the simulation, the micrometer-sized jet from the nozzle was assumed to be a train of droplets with a uniform diameter of droplets based on the experimental setup for the initial test. Sensitivity studies for different diameters were applied to evaluate the possible deviation due to the uncertainty of surface-to-volume ratio. To evaluate the uptake kinetics of SO_2 on the droplet, the mass transfer coefficient, k_{mt}, for gas-phase with interfacial mass transfer of SO_2 on a spherical droplet was expressed as follows:[5]

$$k_{mt} = \left(\frac{R_p^2}{3D_g} + \frac{R_p}{3\alpha_{SO2}} \sqrt{\frac{2\pi M_w}{RT}} \right)^{-1} \quad (12)$$

where R_p is the radius of droplet, D_g is the diffusivity of SO_2 in air and assumed as 0.1 $cm^2\ s^{-1}$, M_w is the molecular weight of SO_2, R is the universal gas constant, T is temperature, and α_{SO2} is the accommodation coefficient of SO_2. To fit the negligible oxidation by H_2O_2 at low pH, a much lower α_{SO2} than the previously reported value was applied as 3×10^{-5} for pH < 3 then increases linearly with pH to 0.11 at pH = 5 and remained constant for pH ≥ 5.[23,24] The concentration of HSO_3^- and SO_3^{2-} inside the droplet was estimated based on the rate constants for the dissociation of aquated SO_2 from our previous study[7] with $k_1 = 3.6 \times 10^6\ s^{-1}$ and $k_2 = 1 \times 10^6\ s^{-1}$. For simplification, the pH of the droplets was assumed to be undisturbed by the dissociation of $SO_2{\cdot}H_2O$ or the formed sulfate. The diffusion of protons in aqueous solution is efficient with a diffusion coefficient of $9.3 \times 10^{-5}\ cm^2\ s^{-1}$ that corresponds to a diffusion length of 10 μm at 1 ms,[25] which is a similar size to diameter of the electrospray jet.

For the sprayed jet, the pH of droplets may be affected by the Kelvin effect and the possible evaporation causing the composition variation, which might lead the pH deviation of droplets from the bulk solution condition. Since the droplets exposed to SO_2 in the air flow was estimated to be in the micrometer size range, the Kelvin effect can be ignored. In the case of evaporation, if the process followed the similar trend as reported by Smith et al.,[26] evaporation would result in 8 μm droplets having a 7% of decrease in volume after 1 ms of reaction time. The resulting pH is estimated to increase approximately 0.03 pH units using the E-AIM thermodynamic models.[27,28] The pH of droplets over the reaction zone without the contribution of SO_2 was then assumed to be the same as the bulk solution.

In this study, various amounts of H_2O_2 were added to the bulk solution to provide a set of standard reactions to retrieve the required adjustment for the correlation of the assumed droplet size and exposure time based on the known oxidation rate constant of HSO_3^- by H_2O_2 as stated in eq 8. The droplet size and exposure time are the necessary parameters to retrieve the efficiency of interfacial surface oxidation mechanisms. At a solution injection rate of 5 $\mu L\ min^{-1}$, the jet diameter initially formed from the nozzle was within several micrometers with a flow speed of a few m/s.[29] The reaction time was estimated to be ∼1 ms with the gas stream, and corresponding to a droplet diameter of 8 μm for a partial pressure of SO_2, P_{SO_2}, of 2000 ppm to obtain better fitting for the sulfate formation rate via the oxidation of $H_2O_2(aq)$. The parameters of the droplets size at 8 μm and reaction time at 1 ms were applied to simulate the sulfate formation via interfacial surface reactions. A decrease of P_{SO2} corresponds to an increase in reaction time but has no influence on the retrieval of the efficiency of interfacial surface oxidation. This experimental setting corresponds to 1.0 h of reaction time under regular ambient conditions of 3 ppb of SO_2, if similar interfacial oxidation kinetics hold in the low concentration region.

The interfacial surface reaction rate ($R_{in,droplet}$) in one spherical droplet with a radius of R_p was assumed to be proportional to the collision frequency of the SO_2 gas molecules on the droplet surfaces with a reaction efficiency factor of q as shown in the following equation:

$$R_{in,droplet} = 1/4\bar{c}nq\ (4\pi R_p^2)\ (molecules\ droplet^{-1}\ s^{-1}) \quad (13)$$

where $\bar{c} = (8RT/\pi M_w)^{1/2}$ the mean speed of molecule, and n is the number density of $SO_2(g)$ at molecules/m^3-air. After the division by the volume of the droplet and Avogadro's constant (N_A), $R_{in,droplet}$ can be converted to units of M/s, the same units as $R_{H_2O_2,droplet}$ in eq 8. Overall, SO_2 molecules collide on the droplets can either deflect back to the gas phase, accommodate into the aqueous phase, or proceed to undergo interfacial surface reactions.

3. RESULTS AND DISCUSSIONS

Significant levels of $SO_3^{-\bullet}$, $SO_4^{-\bullet}$, and HSO_4^- were observed at pH < 3.5 in the absence of an added oxidant except for oxygen, which was likely present in the influent carrier gas or dissolved in the aqueous solution as reported in our previous study.[7] The sulfite radical anion, $SO_3^{-\bullet}$, is likely generated by

DOI: 10.1021/acs.est.8b01391
Environ. Sci. Technol. 2018, 52, 9079−9086

direct interfacial electron transfer within water clusters that constitute the interfacial air−water layer to directly yield the sulfite radical,

$$H_2O + SO_2 + O_2 \rightarrow SO_3^{-\bullet} + O_2^{-\bullet} + 2H^+ \quad (14)$$

which then initiates the free radical chain reactions to form sulfate (vide supra). Due to the limited uptake of SO_2 in the acidic aqueous phase,[23,24] the observed results suggest that SO_2 is not in the HSO_3^- form to precede the interfacial surface reactions. To investigate the impact of such interfacial surface reactions, the amount of sulfate formed was quantified using the intensity response of standard Na_2SO_4 solutions as a function of pH in ESI-MS. The interfacial surface oxidation efficiency, q, in eq 13 was derived by comparing the quantity of sulfate from this interfacial surface oxidation with that from the well-known H_2O_2 oxidation kinetics.

3.1. Intensity Response of Sulfate to pH. H_2SO_4 is a strong diacid with a value of $K_{a1} > 10^3$ ($pK_{a1} < -3$) while $K_{a2} = 1.3 \times 10^{-2}$ ($pK_{a2} \approx 1.9$). The fraction of HSO_4^- included in the observed total S(VI) signal should be the highest at pH ≤ 1.9 based on the dissociation constants. However, the intensity response of HSO_4^- ($m/e = 97$), I_{97}, in ESI-MS generated from 0.1 mM Na_2SO_4 solution increases significantly at pH ≥ 3 and then approaches to a steady intensity at pH ≥ 5 as shown in Figure 2. The intensity trend as a function of pH is similar to

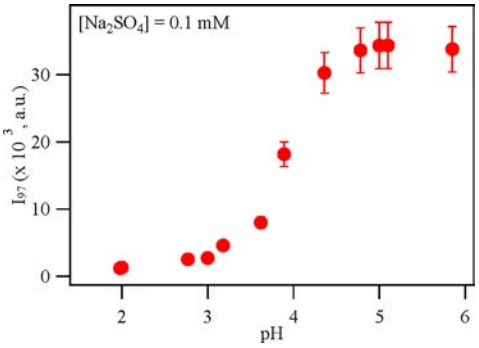

Figure 2. Intensity variation of HSO_4^- ($m/e = 97$) as a function of pH probed using ESI-MS. Condition: $[Na_2SO_4] = 0.1$ mM.

the response of hexanoate ion generated from the hexanoic acid solution[30] but the properties of hexanoic acid and sulfuric acid are very different. The expected decreasing trend of I_{97} from ESI-MS starting at pH ≥ 3 was not observed likely due to the protonation of SO_4^{2-}. As the ions were formed in the spraying chamber, the charge density of SO_4^{2-} might be too high to be stable in the gas phase and the proton transfer from water to SO_4^{2-} happens during the spray-drying processes.[31,32] Even with the significant charge transfer between water and SO_4^{2-}, I_{97} should be the same for the whole pH range studied. The significant higher intensity of I_{97} at pH ≥ 3 might suggest a complicated intensity response of S(VI) to pH in addition to the possible unique interfacial properties such as a different interfacial acidity compared to the bulk solution as discussed in other studies.[30,33] If the charge transfer between H_2O and SO_4^{2-} is sufficient to explain the trend for pH ≥ 5, then the observed lower I_{97} at pH ≤ 4 might be explained with a significantly higher surface acidity than the bulk condition, as suggested that the outer surface of water has Brønsted neutral at pH ≈ 3 rather than at pH = 7.[30] The observed oligomerization of isoprene,[34] usually required under concentrated sulfuric acid solution, on the droplets with pH ≤ 3.6 also suggest the possibility of higher acidity or different reactivity over the interfacial region than the bulk condition. The unique properties of the acidic surface region could promote special chemical reactions such as eq 14.

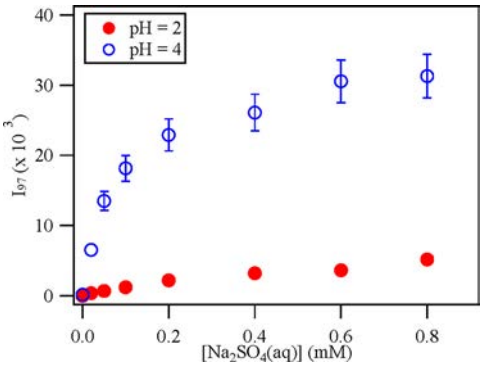

Figure 3. Intensity of HSO_4^-, I_{97}, as a function of $[Na_2SO_4]$ for conditions of pH = 2 and 4.

Due to the pH-dependent response of sulfate intensity, $I_{97}(HSO_4^-)$ as a function of $[Na_2SO_4]$ and pH was determined as a calibration for measuring the quantity of sulfate formed under experimental conditions. At a given pH, I_{97} increases linearly with $[Na_2SO_4(aq)]$ for $[Na_2SO_4(aq)] \leq 100$ μM; while the response becomes nonlinear at higher concentrations as shown in Figure 3. The quantification of sulfate was then based on an interpolation method for I_{97} as a function of concentration at different pH conditions.

3.2. Quantification of the Sulfate Formation Rate. Using the sulfate calibration, the data in Figure 4 show the

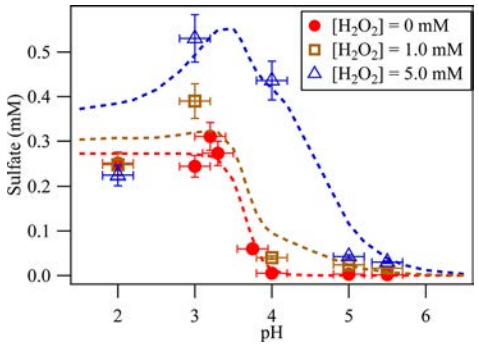

Figure 4. Formation of $[HSO_4^-]$ as a function of pH for conditions of $[H_2O_2] = 0$, 1.0, and 5.0 mM. Data points are measurements while the dashed lines are obtained from simulations as described in the text.

formed sulfate concentration, [S(VI)], as a function of pH for different $[H_2O_2]$. [S(VI)] from the interfacial surface reactions at pH ≥ 4 is negligible as compared with that generated from the oxidation of S(IV) by H_2O_2. For a given pH with less significant interfacial surface reactions, [S(VI)] as a function of $[H_2O_2]$ was linear as shown in Figure 5 for pH = 4. The linear trend suggests that the oxidation of SO_2 via H_2O_2 oxidation in this system is a pseudo-first-order kinetic process in which the sulfate formation rate is linearly proportional to $[H_2O_2]$. The available $[HSO_3^-]$ in the droplets was sufficiently high without a significant concentration decrease due to consumption by oxidation or acidity changes during the reaction time (~1 ms).

DOI: 10.1021/acs.est.8b01391
Environ. Sci. Technol. 2018, 52, 9079−9086

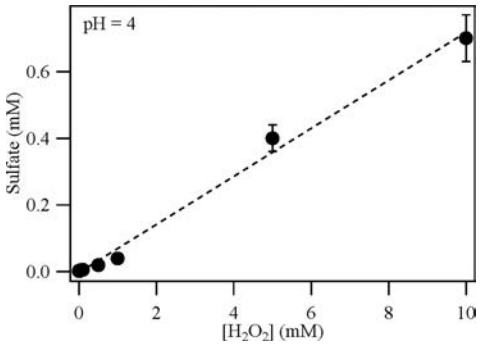

Figure 5. $[HSO_4^-]$ formation as a function of $[H_2O_2]$ at pH = 4.

To simulate the observed sulfate quantity, eq 8 with the droplet size, reaction time and SO_2 partial pressure, was applied to fit the experimental results with $[HSO_3^-]$ estimated from the uptake of SO_2 on the droplets (eq 12) and the dissociation rate constants given in eqs 9−11. For the simulation of interfacial surface reactions, q as a function of $[H^+]$ was manually adjusted to provide a good fitting of [S(VI)] for the experimental results at $[H_2O_2]$ = 0 as expressed as follows:

$$q = \frac{5.6 \times 10^{-5}[H^+]^{3.7}}{[H^+]^{3.7} + 10^{-13.5}} \quad (15)$$

and shown in Figure 6 based on the parameters of the droplets size at 8 μm, a reaction time of 1 ms, and a P_{SO2} of 2000 ppm.

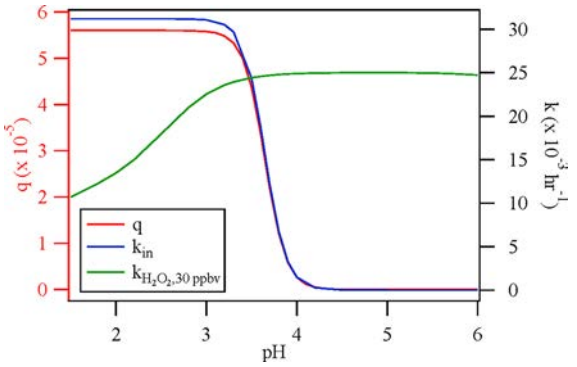

Figure 6. Derived reaction efficiency factor, q, and the two rate constants (k_{in} and $k_{H_2O_2,30\ ppb}$) as a function of pH (q corresponds to the left y-axes while the rate constants to the right y-axes).

The sulfate quantity as a function of pH at different $[H_2O_2]$ for both measurement and simulation is summarized in Figure 4. The combination of interfacial surface reactions with O_2 and the contribution by H_2O_2 oxidation, i.e., $R_{in,droplet} + R_{H_2O_2,droplet}$, provides a comparable result with the measurements at different pH. However, the reported interfacial surface reaction rate is a lower limit, since the applied carrier gas and nebulizer gas is nitrogen, which led to a very low oxygen content in the spray chamber. In our previous study,[7] a switch of carrier gas from nitrogen to air was shown to enhance the intensity of formed sulfate by a factor of 3. This type enhancement was not taken into account in the current study for simplification.

Due to different uptake efficiencies among the different size of droplets, the required exposure time (t_e) as a function of droplet size is summarized in Figure 7 to obtain the same level of sulfate formation as obtained via the oxidation of S(IV) by

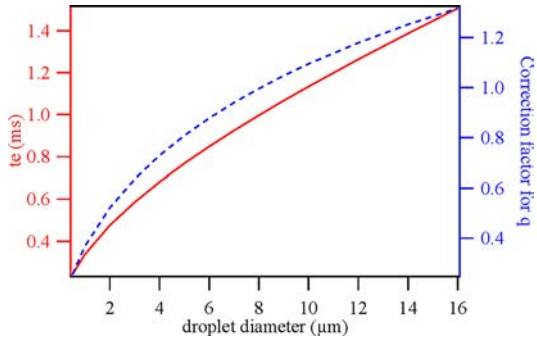

Figure 7. Required exposure time, t_e, (solid line) as a function of droplet diameter to form the estimated sulfate quantity for reaction conditions of $[H_2O_2]$ = 5.0 mM and pH = 4. The dashed line is the correction factor as a function of droplet diameter required to correct the q value.

H_2O_2. For droplet diameters in the range of 1−16 μm, t_e was estimated to be in the range of 0.3−1.5 ms, which is consistent with our previous study[7] but much longer than the earlier reported values, ≤10 μs.[30,33] A shorter exposure time is required for a smaller size of droplets due to the higher surface-to-volume ratio. In our reported q values, the diameter of the droplets was assumed to be 8 μm, which corresponds to a t_e of 1 ms. However, the uncertainty in droplet diameters can cause the deviation of q with a correction factor in the range of 0.3−1.3 for jet diameters of 1−16 μm as shown in Figure 7. This correction factor is within the same order and may be negligible or higher than 1 as the oxygen concentration taken into account.

3.3. Influence of Acidification. The applied SO_2 was significantly high and may induce the acidification of the droplets, which in turn may impact SO_2 uptake and the rate of oxidation, especially at higher pH.[23] The influence of hydronium is similar to the nitrate effect in the N_2O_5 uptake in solution as reported by Wahner et al.,[35] and Bertram and Thornton.[36] Given the applied conditions and a reaction time of 1 ms, an extra 0.001 M of hydronium might be expected for pH > 4. This will affect droplets with higher pH values but will have a negligible influence on droplets having pH < 3. However, a possible enhancement of the interfacial reaction due to this pH decreasing was observed negligible for pH > 4 (Figure 4) and this result might suggest such acidification might be overestimated in the current calculation. On the basis of the results of negligible interfacial reaction at pH > 4, the acidification for the applied system was likely to be less than $10^{-4.5}$ M of hydronium increasing due to the uptake of SO_2 in the study. For current model calculation, the acidification was assumed to be negligible; this specific assumption would effectively result in a higher HSO_3^- concentration coupled with a smaller value for the term, $[H^+]/(1 + 13 \times [H^+])$, in the rate eq 8. If the acidification were taken account, then it should lead to a lower HSO_3^- concentration coupled with a higher value for $[H^+]/(1 + 13 \times [H^+])$; this effectively would require a new calibration curve. Thus, acidification may result in a higher uncertainty for the rate of sulfate formation at pH > 4.5. Due to the opposite impact of pH on the uptake of SO_2 and how it affects to the value of $[H^+]/(1 + 13 \times [H^+])$ along with the pH-dependent sulfate calibration curve, the observed sulfate formation rate would be higher for pH > 4. The effect of enhanced acidification may result in a larger bias for high

DOI: 10.1021/acs.est.8b01391
Environ. Sci. Technol. 2018, 52, 9079−9086

pH conditions, but may not impact the derived rate efficiency trend, which is sensitive at the lower pH.

3.4. Comparison of Different Pathways for Sulfate Formation in Box Model. To compare the efficiency of this surface reaction to the H_2O_2 oxidation pathway, eq 8 was modified to have a rate constant, $k_{H_2O_2}$, as follows:

$$R_{H_2O_2} = 7.45 \times 10^7 [HSO_3^-][H_2O_2(aq)]([H^+]/(1 + 13 \times [H^+])) \times N_A \times V_{aerosol}(\text{molecules m}^{-3}\text{s}^{-1}) = k_{H_2O_2} n(\text{molecules m}^{-3}\text{s}^{-1}) \quad (16)$$

where $V_{aerosol}$ is the total aerosol volume per m^3 of air, and $k_{H_2O_2}$ is the pseudo-first-order reaction rate constant, which is proportional to $[H_2O_2]$. The oxidation rate due to the interfacial surface reaction is then estimated as follows:

$$R_{in} = 1/4\bar{c}nqA \ (\text{molecules m}^{-3}\text{s}^{-1}) = k_{in} n \ (\text{molecules m}^{-3}\text{s}^{-1}) \quad (17)$$

where A is the surface area concentration of aerosol particles in air, m^2/m^3-air and $k_{in} = 4.55\ T^{1/2}\ q\ A\ (s^{-1})$ is the reaction rate constant. In a box model, for a given ambient condition with an aerosol mass concentration of 50 $\mu g/m^3$ (including the water content), a composition density of 1 g cm^{-3}, a mode size at 100 nm, and a geometric standard deviation of 1.5, the rate constants, k_{in} and $k_{H_2O_2,30\ ppb}$ (rate constant for a H_2O_2 partial pressure fixed at 30 ppbv) as a function of pH can be evaluated. As shown in Figure 6, k_{in} at pH < 3.5 is higher than $k_{H_2O_2,30\ ppb}$ at pH > 3, which is at least one order higher than the usual atmospheric partial pressure of H_2O_2 (1−3 ppb)[37] even with a possible q deviation taken into account. With the additional contribution of the oxygen concentration in a regular atmospheric condition compared to the spray chamber, k_{in} would be at least three times higher than this reported value.[7] According to this simple box-model analysis, the interfacial surface reaction between S(IV) and O_2 on aquated acidic aerosols could provide a significant oxidation pathway for SO_2 conversion to SO_4^{2-}. An efficient interfacial surface reaction may be the combined result of a lower activation energy under acidic conditions at the air−water interface, preferred molecule orientation resulting from the water structure right at the air−water interface, and a variation in reactivity with pH on the aquated aerosol surfaces.[7−9,38−40]

4. ATMOSPHERIC IMPLICATIONS

In this study, the heterogeneous reactions involving the conversion of S(IV) to S(VI) on the interfacial surface region were determined with a pH-dependent efficiency factor of $5.6 \times 10^{-5}[H^+]^{3.7}/([H^+]^{3.7}+10^{-13.5})$ based on our specific experimental setup employing the well-studied reaction kinetics of SO_2 oxidation by $H_2O_2(aq)$. If similar oxidation kinetics obtained in this study holds for the ambient atmospheric conditions, then interfacial surface reactions can enhance the net sulfate formation rate in the atmosphere significantly according to a simple box-model calculation with acidic aquated aerosol particles. Whiteaker and Prather reported on the S(VI) formation in the presence of $SO_3^{-\bullet}$ as wood smoke particles were exposed to a gas mixture containing $SO_2(g)$ for individual particles sampled with an aerosol time-of-flight mass spectrometer.[41] However, their study was mainly focused on the formation of hydroxymethanesulfonate with no further discussion accounting for the observed S(VI) and $SO_3^{-\bullet}$ levels.[41]

By performing thermodynamic calculations for metastable aerosol conditions using E-AIM models,[27,28] the pH of aerosols for a given composition can be estimated for various environmental conditions. In addition to relative humidity, the acidity of aerosols is dependent on the availability of ammonia and the ambient temperature. For example, bisulfate in ambient aerosols can be readily neutralized by the uptake of gas-phase NH_3 or other available alkaline species in the particles. Sulfate related species mainly appear in the submicrometer sized region, which usually has a limited amount of dust content.[42,43] For aerosol particles composed primarily of pure ammonia sulfate, the pH in the aqueous phase particles is often in the range of 4.9 to 5.0 for RH between 40 and 80% and T = 298 K (e.g., activity coefficient corrections for H^+ were taken into account). If the aerosol composition has 0.1% of bisulfate that is not neutralized by ammonia or other alkaline species, then the pH can be reduced to the range of 2.5−3.0, which is in the optimal range to induce efficient interfacial O_2 oxidation of SO_2. For polluted areas, plume generated by burning processes, contain CO, NO_2, organic species, and SO_2. NO_2 can react with OH to form HNO_3, which can partition in the aqueous phase to increase the acidity or be photolyzed back to OH and NO_2. With a reaction rate constant of 2.4×10^{-11} cm^3 $molecule^{-1}$ s^{-1},[5] the HNO_3 formation rate is estimated to be 0.72 pptv s^{-1} at $[OH] = 10^6$ molecules cm^{-3} and $[NO_2]$ = 30 ppbv. If the aerosol particle consists of 0.01% HNO_3 and 99.99% of ammonium sulfate, which corresponds to the mixing ratio of 1−0.4 ppbv of HNO_3 at RH of 80−40%, then the pH of the aquated aerosol can be reduced to 3.8−4.3. Even under these conditions, interfacial surface reactions leading to the conversion of SO_2 to sulfate can take place especially in regions having lower partitioning of NH_3 into the aqueous phase.[44] For example, under actual ambient conditions with a sulfate concentration of 26 $\mu g/m^3$, nitrate = 26 $\mu g/m^3$, total ammonia (i.e., $NH_4^+ + NH_3$) = 32 $\mu g/m^3$, the pH at RH = 56% is estimated to be 2.6 for 298 K and 3.9 for 274 K.[45] It is clear that interfacial surface reactions will play a significant role as the temperature increases and thus provide an important pathway for the sulfate formation during the summer as well.[17] On the basis of the results presented herein, interfacial surface reactions can play an important role in the heterogeneous atmospheric chemistry. The interfacial surface reactions are overlooked in most atmospheric chemistry models and might provide further insight into alternative reaction pathways, which impact SO_2 oxidation to sulfate in regions of the world using high-sulfur fuel and having particles partially neutralized by ammonia or other alkaline species.

AUTHOR INFORMATION

Corresponding Author

*E-mail: hmhung@ntu.edu.tw (H.-M.H.).

ORCID

Hui-Ming Hung: 0000-0002-6755-6359

Notes

The authors declare no competing financial interest.

ACKNOWLEDGMENTS

Funding for this research was provided by the Ministry of Science and Technology in Taiwan (105-2111-M-002-001 and 106-2111-M-002-007). Additional support was provided by the US National Science Foundation (Grant Number: AGS 1744353). We also appreciate the instrument support provided by Dr. Chau-Chung Han from the Institute of Atomic and

DOI: 10.1021/acs.est.8b01391
Environ. Sci. Technol. 2018, 52, 9079−9086

Molecular Sciences, Academia Sinica. Discussions with Prof. Becky Alexander from the University of Washington during a recent Gordon Research Conference and thermodynamic model discussions with Drs. Shaojie Song and Pengfei Liu of Harvard University, and the constructive comments from the anonymous reviewers are appreciated.

REFERENCES

(1) McMurry, P. H. A review of atmospheric aerosol measurements. *Atmos. Environ.* **2000**, *34* (12−14), 1959−1999.
(2) Finlayson-Pitts, J. B.; Pitts, N. J. J. *Chemistry of the Upper and Lower Atmosphere*; Academic Press: San Diego, 2000.
(3) Richardson, C. B.; Spann, J. F. Heterogeneous and multiphase chemistry in the troposphere. *J. Aerosol Sci.* **1984**, *15* (5), 563−571.
(4) Pilinis, C.; Seinfeld, J. H.; Grosjean, D. Water-content of atmospheric aerosols. *Atmos. Environ.* **1989**, *23* (7), 1601−1606.
(5) Seinfeld, J. H.; Pandis, S. N. *Atmospheric Chemistry and Physics*; Wiley: New York, 2006.
(6) Hoffmann, M. R.; Edwards, J. O. Kinetics of oxidation of sulfite by hydrogen-peroxide in acidic solution. *J. Phys. Chem.* **1975**, *79* (20), 2096−2098.
(7) Hung, H.-M.; Hoffmann, M. R. Oxidation of Gas-Phase SO_2 on the Surfaces of Acidic Micro-Droplets: Implications for Sulfate and Sulfate Radical Anion Formation in the Atmospheric Liquid Phase. *Environ. Sci. Technol.* **2015**, *49* (23), 13768−13776.
(8) Hegg, D. A.; Hobbs, P. V. Oxidation of sulfur dioxide in aqueous systems with particular reference to the atmosphere. *Atmos. Environ.* **1978**, *12* (1−3), 241−253.
(9) Larson, T. V.; Horike, N. R.; Harrison, H. Oxidation of sulfur dioxide by oxygen and ozone in aqueous-solution - kinetic study with significance to atmospheric rate processes. *Atmos. Environ.* **1978**, *12* (8), 1597−1611.
(10) Clarke, A. G.; Radojevic, M. Authors' reply. *Atmos. Environ.* **1983**, *17* (9), 1857−1858.
(11) Radojevic, M. On the discrepancy between reported studies of the uncatalysed aqueous oxidation of SO_2 by O_2. *Environ. Technol. Lett.* **1984**, *5* (12), 549−566.
(12) McKay, H. A. C. The atmospheric oxidation of sulphur dioxide in water droplets in presence of ammonia. *Atmos. Environ.* **1971**, *5* (1), 7−14.
(13) Wang, Y.; Zhang, Q.; Jiang, J.; Zhou, W.; Wang, B.; He, K.; Duan, F.; Zhang, Q.; Philip, S.; Xie, Y. Enhanced sulfate formation during China's severe winter haze episode in January 2013 missing from current models. *J. Geophys. Res.-Atmos.* **2014**, *119* (17), 10425−10440.
(14) Zheng, B.; Zhang, Q.; Zhang, Y.; He, K. B.; Wang, K.; Zheng, G. J.; Duan, F. K.; Ma, Y. L.; Kimoto, T. Heterogeneous chemistry: a mechanism missing in current models to explain secondary inorganic aerosol formation during the January 2013 haze episode in North China. *Atmos. Chem. Phys.* **2015**, *15* (4), 2031−2049.
(15) Zheng, G. J.; Duan, F. K.; Su, H.; Ma, Y. L.; Cheng, Y.; Zheng, B.; Zhang, Q.; Huang, T.; Kimoto, T.; Chang, D.; Pöschl, U.; Cheng, Y. F.; He, K. B. Exploring the severe winter haze in Beijing: the impact of synoptic weather, regional transport and heterogeneous reactions. *Atmos. Chem. Phys.* **2015**, *15* (6), 2969−2983.
(16) Wang, G.; Zhang, R.; Gomez, M. E.; Yang, L.; Levy Zamora, M.; Hu, M.; Lin, Y.; Peng, J.; Guo, S.; Meng, J.; Li, J.; Cheng, C.; Hu, T.; Ren, Y.; Wang, Y.; Gao, J.; Cao, J.; An, Z.; Zhou, W.; Li, G.; Wang, J.; Tian, P.; Marrero-Ortiz, W.; Secrest, J.; Du, Z.; Zheng, J.; Shang, D.; Zeng, L.; Shao, M.; Wang, W.; Huang, Y.; Wang, Y.; Zhu, Y.; Li, Y.; Hu, J.; Pan, B.; Cai, L.; Cheng, Y.; Ji, Y.; Zhang, F.; Rosenfeld, D.; Liss, P. S.; Duce, R. A.; Kolb, C. E.; Molina, M. J. Persistent sulfate formation from London Fog to Chinese haze. *Proc. Natl. Acad. Sci. U. S. A.* **2016**, *113* (48), 13630−13635.
(17) Huang, X.; Song, Y.; Zhao, C.; Li, M.; Zhu, T.; Zhang, Q.; Zhang, X. Pathways of sulfate enhancement by natural and anthropogenic mineral aerosols in China. *J. Geophys. Res.-Atmos.* **2014**, *119* (24), 14165−14179.
(18) Li, L.; Hoffmann, M. R.; Colussi, A. J. The Role of Nitrogen Dioxide in the Production of Sulfate during Chinese Haze-Aerosol Episodes. *Environ. Sci. Technol.* **2018**, *52* (5), 2686−2693.
(19) Prince, A. P.; Kleiber, P.; Grassian, V. H.; Young, M. A. Heterogeneous interactions of calcite aerosol with sulfur dioxide and sulfur dioxide-nitric acid mixtures. *Phys. Chem. Chem. Phys.* **2007**, *9* (26), 3432−3439.
(20) Enami, S.; Hoffmann, M. R.; Colussi, A. J. In situ mass spectrometric detection of interfacial intermediates in the oxidation of RCOOH(aq) by gas-phase OH-radicals. *J. Phys. Chem. A* **2014**, *118* (23), 4130−4137.
(21) Colussi, A. J.; Enami, S.; Yabushita, A.; Hoffmann, M. R.; Liu, W.-G.; Mishra, H.; Goddard, W. A., III Tropospheric aerosol as a reactive intermediate. *Faraday Discuss.* **2013**, *165*, 407−420.
(22) McArdle, J. V.; Hoffmann, M. R. Kinetics and mechanism of the oxidation of aquated sulfur dioxide by hydrogen peroxide at low pH. *J. Phys. Chem.* **1983**, *87* (26), 5425−5429.
(23) Jayne, J. T.; Davidovits, P.; Worsnop, D. R.; Zahniser, M. S.; Kolb, C. E. Uptake of SO_2(g) by aqueous surfaces as a function of pH - The effect of chemical-reaction at the interface. *J. Phys. Chem.* **1990**, *94* (15), 6041−6048.
(24) Zhang, J. X.; Aker, P. M. Charge-enhanced uptake of SO_2 at the water/air interface. *Chem. Phys. Lett.* **1998**, *298* (1−3), 183−188.
(25) Pines, E.; Huppert, D.; Agmon, N. Geminate recombination in excited-state proton-transfer reactions: Numerical solution of the Debye-Smoluchowski equation with backreaction and comparison with experimental results. *J. Chem. Phys.* **1988**, *88* (9), 5620−5630.
(26) Smith, J. N.; Flagan, R. C.; Beauchamp, J. L. Droplet Evaporation and Discharge Dynamics in Electrospray Ionization. *J. Phys. Chem. A* **2002**, *106* (42), 9957−9967.
(27) Clegg, S. L.; Brimblecombe, P.; Wexler, A. S. Thermodynamic model of the system H^+-NH_4^+-Na^+-SO_4^{2-}-NO_3^--Cl^--H_2O at 298.15 K. *J. Phys. Chem. A* **1998**, *102* (12), 2155−2171.
(28) http://www.aim.env.uea.ac.uk/aim/aim.php.
(29) Wortmann, A.; Kistler-Momotova, A.; Zenobi, R.; Heine, M. C.; Wilhelm, O.; Pratsinis, S. E. Shrinking Droplets in Electrospray Ionization and Their Influence on Chemical Equilibria. *J. Am. Soc. Mass Spectrom.* **2007**, *18* (3), 385−393.
(30) Mishra, H.; Enami, S.; Nielsen, R. J.; Stewart, L. A.; Hoffmann, M. R.; Goddard, W. A., III; Colussi, A. J. Bronsted basicity of the air-water interface. *Proc. Natl. Acad. Sci. U. S. A.* **2012**, *109* (46), 18679−18683.
(31) Fenn, J. B.; Mann, M.; Meng, C. K.; Wong, S. F.; Whitehouse, C. M. Electrospray ionization for mass-spectrometry of large biomolecules. *Science* **1989**, *246* (4926), 64−71.
(32) Fenn, J. B.; Mann, M.; Meng, C. K.; Wong, S. F.; Whitehouse, C. M. Electrospray ionization principles and practice. *Mass Spectrom. Rev.* **1990**, *9* (1), 37−70.
(33) Enami, S.; Hoffmann, M. R.; Colussi, A. J. Proton availability at the air/water interface. *J. Phys. Chem. Lett.* **2010**, *1* (10), 1599−1604.
(34) Enami, S.; Mishra, H.; Hoffmann, M. R.; Colussi, A. J. Protonation and oligomerization of gaseous isoprene on mildly acidic surfaces: Implications for atmospheric chemistry. *J. Phys. Chem. A* **2012**, *116* (24), 6027−6032.
(35) Bertram, T. H.; Thornton, J. A. Toward a general parameterization of N_2O_5 reactivity on aqueous particles: the competing effects of particle liquid water, nitrate and chloride. *Atmos. Chem. Phys.* **2009**, *9* (21), 8351−8363.
(36) Wahner, A.; Mentel, T. F.; Sohn, M.; Stier, J. Heterogeneous reaction of N_2O_5 on sodium nitrate aerosol. *J. Geophys. Res.-Atmos.* **1998**, *103* (D23), 31103−31112.
(37) Hua, W.; Chen, Z. M.; Jie, C. Y.; Kondo, Y.; Hofzumahaus, A.; Takegawa, N.; Chang, C. C.; Lu, K. D.; Miyazaki, Y.; Kita, K.; Wang, H. L.; Zhang, Y. H.; Hu, M. Atmospheric hydrogen peroxide and organic hydroperoxides during PRIDE-PRD'06, China: their concentration, formation mechanism and contribution to secondary aerosols. *Atmos. Chem. Phys.* **2008**, *8* (22), 6755−6773.

DOI: 10.1021/acs.est.8b01391
Environ. Sci. Technol. 2018, 52, 9079−9086

(38) Tarbuck, T. L.; Richmond, G. L. Adsorption and reaction of CO_2 and SO_2 at a water surface. *J. Am. Chem. Soc.* **2006**, *128* (10), 3256−3267.
(39) Shamay, E. S.; Valley, N. A.; Moore, F. G.; Richmond, G. L. Staying hydrated: the molecular journey of gaseous sulfur dioxide to a water surface. *Phys. Chem. Chem. Phys.* **2013**, *15* (18), 6893−6902.
(40) Baer, M.; Mundy, C. J.; Chang, T. M.; Tao, F. M.; Dang, L. X. Interpreting vibrational sum-frequency spectra of sulfur dioxide at the air/water Interface: a comprehensive molecular dynamics study. *J. Phys. Chem. B* **2010**, *114* (21), 7245−7249.
(41) Whiteaker, J. R.; Prather, K. A. Hydroxymethanesulfonate as a tracer for fog processing of individual aerosol particles. *Atmos. Environ.* **2003**, *37* (8), 1033−1043.
(42) Hung, H.-M.; Hsu, C.-H.; Lin, W.-T.; Chen, Y.-Q. A Case Study of Single Hygroscopicity Parameter and its Link to the Functional Groups and Phase Transition for Urban Aerosols in Taipei City. *Atmos. Environ.* **2016**, *132*, 240−248.
(43) Tian, S.; Pan, Y.; Liu, Z.; Wen, T.; Wang, Y. Size-resolved aerosol chemical analysis of extreme haze pollution events during early 2013 in urban Beijing, China. *J. Hazard. Mater.* **2014**, *279*, 452−460.
(44) Guo, H. Y.; Weber, R. J.; Nenes, A. High levels of ammonia do not raise fine particle pH sufficiently to yield nitrogen oxide-dominated sulfate production. *Sci. Rep.* **2017**, *7*, 12109.
(45) Song, S.; Gao, M.; Xu, W.; Shao, J.; Shi, G.; Wang, S.; Wang, Y.; Sun, Y.; McElroy, M. B. Fine particle pH for Beijing winter haze as inferred from different thermodynamic equilibrium models. *Atmos. Chem. Phys.* **2018**, *18* (10), 7423−7438.

DOI: 10.1021/acs.est.8b01391
Environ. Sci. Technol. 2018, 52, 9079−9086